

1 **Title page**

2 Title: Large uncertainty in carbon uptake potential of land-based climate-change mitigation
3 efforts

4 Running head: Large uncertainty in carbon uptake potential

5 List of authors: Andreas Krause¹, Thomas A. M. Pugh^{1,2}, Anita D. Bayer¹, Wei Li³, Felix
6 Leung⁴, Alberte Bondeau⁵, Jonathan C. Doelman⁶, Florian Humpenöder⁷, Peter Anthoni¹,
7 Benjamin L. Bodirsky⁷, Philippe Ciais³, Christoph Müller⁷, Guillermo Murray-Tortarolo⁴,
8 Stefan Olin⁸, Alexander Popp⁷, Stephen Sitch⁴, Elke Stehfest⁶, Almut Arneth¹

9 Institute or laboratory of origin: ¹Karlsruhe Institute of Technology, Institute of Meteorology
10 and Climate Research – Atmospheric Environmental Research (IMK-IFU), Kreuzeckbahnstr.
11 19, 82467 Garmisch-Partenkirchen, Germany

12 ²School of Geography, Earth & Environmental Sciences and Birmingham Institute of Forest
13 Research, University of Birmingham, B15 2TT, United Kingdom

14 ³Laboratoire des Sciences du Climat et l'Environnement, CEA-CNRS-UVSQ, Gif-sur-Yvette,
15 France

16 ⁴College of Life and Environmental Sciences, University of Exeter, Exeter, United Kingdom

17 ⁵Institut Méditerranéen de Biodiversité et d'Ecologie marine et continentale (Mediterranean
18 Institute for Biodiversity and Ecology, IMBE), Aix-en-Provence, France

19 ⁶Department of Climate, Air and Energy, Netherlands Environmental Assessment Agency
20 (PBL), PO Box 30314, 2500 GH The Hague, Netherlands

21 ⁷Potsdam Institute for Climate Impact Research (PIK), Telegrafenberg, PO Box 60 12 03,
22 14412 Potsdam, Germany

23 ⁸Department of Physical Geography and Ecosystem Science, Lund University, 22362 Lund,
24 Sweden

Corresponding author's telephone and email details: ++49 8821 183186,
andreas.krause@kit.edu

Keywords: carbon dioxide removal, negative emissions, land-based mitigation, BECCS,
avoided deforestation and afforestation

Paper type: Primary Research Article

Abstract

Most climate mitigation scenarios involve negative emissions, especially those that aim to limit global temperature increase to 2°C or less. However, the carbon uptake potential in land-based climate change mitigation efforts is highly uncertain. Here, we address this uncertainty by using two land-based mitigation scenarios from two land-use models (IMAGE and MAgPIE) as input to four dynamic global vegetation models (DGVMs; LPJ-GUESS, ORCHIDEE, JULES, LPJmL). Each of the four combinations of land-use models and mitigation scenarios aimed for a cumulative carbon uptake of ~130 GtC by the end of the century, achieved either via the cultivation of bioenergy crops combined with carbon capture and storage (BECCS) or avoided deforestation and afforestation (ADAFF).

Results suggest large uncertainty in simulated future land demand and carbon uptake rates, depending on the assumptions related to land use and land management in the models. Total cumulative carbon uptake in the DGVMs is highly variable across mitigation scenarios, ranging between 19 and 130 GtC by year 2099. Only one out of the 16 combinations of mitigation scenarios and DGVMs achieves an equivalent or higher carbon uptake than achieved in the land-use models. The large differences in carbon uptake between the DGVMs and their discrepancy against the carbon uptake in IMAGE and MAgPIE are mainly due to

different model assumptions regarding bioenergy crop yields, and due to the simulation of soil carbon response to land-use change. Differences between land-use models and DGVMs regarding forest biomass and the rate of forest regrowth also have an impact, albeit smaller, on the results. Given the low confidence in simulated carbon uptake for a given land-based mitigation scenario, and that negative emissions simulated by the DGVMs are typically lower than assumed in scenarios consistent with the 2°C target, relying on negative emissions to mitigate climate change is a highly uncertain strategy.

Introduction

“Negative emissions”, i.e. the removal of carbon dioxide (CDR) from the atmosphere, is an important concept for climate change mitigation (Lenton and Vaughan, 2009). Scenarios based on land-use (LU) models or Integrated Assessment Models (IAMs) tend to achieve an end-of-century warming goal at or below 2°C only through negative emissions which commence within the next 1-2 decades, and then increase and are sustained at considerable rates during the second half of the 21st century (Anderson and Peters, 2016, Fuss *et al.*, 2014, Gasser *et al.*, 2015, Riahi *et al.*, 2017, Rogelj *et al.*, 2015, Sanderson *et al.*, 2016, Smith *et al.*, 2016a). So far, negative emissions represented in IAMs are mainly land-based options (Popp *et al.*, 2017, Popp *et al.*, 2014b).

IAMs currently focus on two land-based CDR technologies which both utilize the carbon (C) uptake by plants via photosynthesis. One is large-scale cultivation of crops or trees for bioenergy and capturing the C released upon combustion for long-term storage in geologic formations (BECCS). The other is to maintain or increase terrestrial C stocks via avoided deforestation and afforestation/reforestation (ADAFF). These are the two most widely-used options in IAMs to achieve negative emissions because they do not have to rely on the

development of new, large-scale technology (ADAFf), or are regarded as the most prolific option with the capability to supply energy (BECCS) (Humpenöder *et al.*, 2014, Smith *et al.*, 2016a). However, the land demand/availability of these approaches is highly uncertain (Boysen *et al.*, 2017a, Popp *et al.*, 2017), and their potential to remove significant amounts of C from the atmosphere is regarded as controversial (Fuss *et al.*, 2014). Additionally, conflicts with other LU, associated supply of ecosystem services, and maintenance/enhancement of biodiversity are highly likely (Krause *et al.*, 2017, Smith *et al.*, 2016a, Williamson, 2016). Considering typical time frames of decades involved in the planning and establishment of climate mitigation projects, the quantification of their uncertainties in terms of achievable CDR is important to inform policy makers about practicality and risks.

Here, we address the uncertainty of C uptake potential from land-based climate change mitigation by using projections of future land-use change (LUC) from one IAM (IMAGE) and one socio-economic LU model (MAGPIE; for simplicity we refer to IMAGE and MAGPIE as land-use models - LUMs - in the following) as input to four dynamic global vegetation models (DGVMs; LPJ-GUESS, ORCHIDEE, JULES, LPJmL). In these scenarios, C uptake is achieved either via BECCS or via ADAFF. The cumulative additional C uptake target in each mitigation LUC scenario is 130 GtC by year 2100 compared to a baseline LUC scenario without additional land-based mitigation (BASE). We analyze total C uptake and the relative contribution of vegetation, soils, and C storage via CCS in the four DGVMs and compare it to the C uptake targeted and achieved in the LUMs.

Materials and methods

Detailed information about the LUMs and the scenarios can be found in Krause *et al.* (2017). In the following we provide a short description of the LUMs and the scenarios.

97 Description of the land-use models

98 The Integrated Model to Assess the Global Environment (IMAGE) is an ecological-
99 environmental model framework simulating the environmental consequences of human
100 activities worldwide (Stehfest *et al.*, 2014).

101 The Model of Agricultural Production and its Impact on the Environment (MAGPIE) is a
102 global LU and agro-food system model. It optimizes spatial-explicit LU patterns and
103 intensification levels to satisfy a given food, feed, material, and bioenergy demand at minimal
104 production costs (Lotze-Campen *et al.*, 2008, Popp *et al.*, 2014a).

105 Climate change and CO₂ impacts on forest growth and crop yields are accounted for in the
106 LUMs. The LPJmL DGVM (Bondeau *et al.*, 2007) represents the crop/vegetation sub-model
107 in both IMAGE (where it is dynamically coupled) and MAGPIE (where it provides potential C
108 stocks, crop yields, irrigation water requirements, and blue water availability as input data).
109 We also use an offline version of LPJmL as one of our four DGVMs which differs from the
110 versions used in the LUMs mainly by not considering technological yield increases in the
111 future.

112

113 Land-use scenarios

114 Both LUMs harmonized their pasture and cropland LU patterns to the HYDE 3.1 dataset
115 (Klein Goldewijk *et al.*, 2011) in the years 2005 (IMAGE) or 1995 (MAGPIE) to create a
116 continuous historical-to-future time series. The simulation period was 1970-2100 for IMAGE
117 and 1995-2100 for MAGPIE, with LUC scenarios starting to diverge in year 2005. The spin-
118 up in IMAGE was set to 700 years with natural vegetation cover followed by 300 years with

year 1970 land-cover map, climate and CO₂. In MAgPIE, potential C densities from LPJmL were used as initial (1995) values, with agricultural vegetation and litter C set to zero and soil C depleted based on IPCC recommendations to account for real land cover at the start of the simulation period (Humpenöder *et al.*, 2014). Socioeconomic developments as input to the LUMs were based on SSP2 (Popp *et al.*, 2017). Food production in the mitigation scenarios was maintained on the same levels as in BASE.

With respect to the rate of forest regrowth in the ADAFF scenarios, MAgPIE parameterizes managed afforestation by climate region specific S-shaped growth curves towards potential forest biomass, and litter and soil C recovering within 20 years (Humpenöder *et al.*, 2014). In contrast, forest regrowth in IMAGE is dynamically simulated by LPJmL, which is a sub-component of IMAGE. This means that similar C uptake rates following afforestation are to be expected for IMAGE and the stand-alone LPJmL DGVM. Forest regrowth in IMAGE partly takes place on degraded forest lands, which are assumed to be completely deforested (Doelman *et al.*, 2018).

The degraded forest land-cover class was implemented in IMAGE due to a mismatch between deforestation rates reported by the FAO's 2015 Forest Resource Assessment (<http://www.fao.org/3/a-i4793e.pdf>, last accessed September 2017) and historical expansions of cropland and pasture area reported by FAO. These differences are assumed to be caused by additional reasons (e.g. unsustainable forestry preventing regrowth of natural forests, mining, or illegal logging) and accounted for by a historically calibrated rate of forest degradation, which is extrapolated into the future (Doelman *et al.*, 2018).

Description of the Dynamic Global Vegetation Models

The LUC scenarios were used as input to four DGVMs: LPJ-GUESS (Olin *et al.*, 2015, Smith *et al.*, 2014), ORCHIDEE (Krinner *et al.*, 2005), JULES (Best *et al.*, 2011, Clark *et al.*, 2011), and LPJmL (Bondeau *et al.*, 2007, Sitch *et al.*, 2003). The models have different heritages; while ORCHIDEE and JULES were developed as land components of global climate models (IPSL and UKESM), LPJ-GUESS and LPJmL were originally designed as stand-alone offline models to simulate vegetation dynamics and associated C and water fluxes. All DGVMs represent vegetation using a number of plant functional types (PFTs), with LPJ-GUESS and LPJmL also representing dedicated crop PFTs. LPJ-GUESS is different from the other DGVMs by its explicit representation of forest demography and by having nitrogen cycling as an additional constraint on ecosystem C processes (in addition to soil water availability which is accounted for in all DGVMs). All DGVMs represent LUC and land management explicitly even though the models differ in terms of implemented processes and level of detail. Table 1 and the extended Table S1 provide an overview of model differences which are important for this study.

Simulation setup

The DGVM simulation period was 1901-2099. DGVMs were first spun up to pre-industrial equilibrium state (1901), recycling 1950-1959 climatology to attain a stable equilibrium of C pools and fluxes in each model using atmospheric CO₂ concentration from 1901 (Meinshausen *et al.*, 2011). Climate from the 1950-1959 period was used for the spin-up because these were the first years in the climate data set, a common practice in this kind of set-up. DGVMs were then applied over the transient period 1901-2099 using transient CO₂ (Meinshausen *et al.*, 2011) and climate data (1950-2099) simulated by the IPSL-CM5A-LR climate model for the representative concentration pathway RCP2.6 from the ISI-MIP project,

bias-corrected as in Hempel et al. (2013). The temperature increase is 2°C by the end of the 21st century relative to the pre-industrial era. The climate data for the spin-up and the 1901-1949 period were randomly taken from the 1950-1959 period. Future atmospheric CO₂ mixing ratio followed the RCP2.6 pathway, peaking at 443 ppmv in year 2052 (Meinshausen *et al.*, 2011). LUC was based on spatially explicit LU maps derived from the LUMs (for the historic period based on HYDE3.1) and translated into the vegetation types of each DGVM (see Table 1). The DGVMs aimed to be as consistent as possible with the LUMs when implementing LU patterns from the LUM scenarios, e.g. for IMAGE scenarios all DGVMs apart from JULES followed the IMAGE assumption of degraded forests being grasslands. Management information (crop types, irrigation, and nitrogen fertilizers) were also provided by the LUMs but were only used by some DGVMs which represented the relevant processes explicitly (Table 1). LPJ-GUESS was the only model being able to use nitrogen fertilizers as provided by the LUMs. Nitrogen application rates (synthetic plus manure) were available from 1970/1995 on. They were derived to match assumed crop yields in the LUMs. A historic hindcast (1901-1969/1901-1994) was calculated based on initial (1970/1995) fertilizer rates from the LUMs and relative changes in the Land-Use Harmonization data set (<http://luh.umd.edu/index.shtml>, see also Krause et al., 2017). The implementation of the LU data into the DGVMs (e.g. mapping to DGVM vegetation types and defining rules by which managed land expands over natural vegetation), land masks, and additional required input variables (e.g. soil characteristics) were left to the responsibility of the individual DGVM groups. Different model structures and implementations of the LU patterns can result e.g. in differences in global forest area in the individual DGVMs (Fig. S1). The spatial resolution of the DGVMs was the same as the resolution of the input data (0.5°x0.5°), except for ORCHIDEE (2°x2°). In total, 24 combinations of DGVMs and LUC scenarios were simulated, including 16 combinations of DGVMs and mitigation LUC scenarios.

191

192 **Results**

193 Land-use scenarios

194 In both LUMs, LUC is generally greater for ADAFF scenarios than for BECCS scenarios
195 (Fig. S2) because the former is simulated with LUMs to be less efficient at CDR than the
196 latter (Humpenöder, et al., 2014). The different C accumulation trajectories in ADAFF (see
197 methods) result in ADAFF activities starting earlier in IMAGE but avoided
198 deforestation/afforestation area being slightly larger in MAgPIE by the end of the century
199 (Figs. S1, S2a,b, Table S2). Forest area by year 2099 is 1040 Mha larger in ADAFF than in
200 BASE for IMAGE and 1103 Mha larger for MAgPIE. For IMAGE, ~42% of this difference in
201 forest area can be attributed to avoided deforestation and 58% to afforestation. For MAgPIE,
202 the corresponding numbers are only 4% for avoided deforestation and 96% for afforestation,
203 emphasizing the much larger role of afforestation compared to avoided deforestation in
204 MAgPIE. The LUMs also differ in terms of land-cover classes affected by ADAFF activities.
205 In IMAGE, forest maintenance and expansion usually takes place on pastures or degraded
206 forests (ADAFF compared to BASE), but in MAgPIE afforestation on abandoned croplands is
207 also relevant, particularly after year 2070 (see Table S2; note that some of the abandoned
208 cropland in MAgPIE ADAFF is not afforested but instead converted to pasture while at other
209 locations pastures are converted to forests, resulting in small net changes in pasture area by
210 the end of the century).

211 The area needed for bioenergy production is mainly taken from natural vegetation in IMAGE
212 but also from existing agricultural land in MAgPIE. IMAGE has a larger bioenergy land
213 demand to fulfil the same CCS target as MAgPIE (Fig. S2c,d). This reflects different
214 modelling approaches: in IMAGE, land allocation for bioenergy cultivation follows a rule-

based approach according to sustainability criteria, implying that only marginal land not needed for food production is available for bioenergy. In MAgPIE, bioenergy and food production compete for fertile land based on a cost minimization procedure. Consequently, average bioenergy yields are lower in IMAGE than in MAgPIE, thereby increasing the required area to deliver the same annual CCS rates.

Present-day carbon pools and future changes in the baseline scenarios

Present-day C pools as simulated by IMAGE and MAgPIE are 440 and 484 GtC in global vegetation, and 1121 and 1981 GtC in the soils (including litter), respectively. The large divergence in soil C between the two LUMs is likely mainly due to the representation of permafrost in MAgPIE. Vegetation C simulated by the DGVMs ranges between 275 and 425 GtC, and soil C between 1315 and 1954 GtC (Fig. S3). For the two non-mitigation BASE scenarios, in all DGVMs except LPJmL the land acts as a net C sink between year 2000 and 2099 (Fig. S3). The magnitude and direction of change in C pools is determined by the DGVM's response to RCP2.6 climate change, CO₂ fertilization, and baseline LUC.

Total carbon uptake in the mitigation scenarios

Total additional C uptake in the mitigation scenarios is here calculated as the sum of changes in vegetation C, litter and soil C, and (relatively negligible) product pool C, plus cumulative CCS (all relative to BASE). While an uptake target of 130 GtC was set in both LUMs, actual C uptake in the LUMs in most cases deviates somewhat from this number. For the ADAFF scenarios, the simplicity of the afforestation implementation in IMAGE was unable to exactly meet the target. In MAgPIE, afforestation decision-making was based on present-day

potential C pools. Potential impacts of climate change on the terrestrial C storage capacity were therefore not considered which leads to a mismatch between intended and actual sequestration. The realized C uptake in ADAFF between year 2005 and 2099 is 141 GtC in IMAGE and 120 GtC in MAgPIE (Figs. 1a,b, 2a). Around 49% of the total C increase in IMAGE ADAFF can be attributed to avoided deforestation and 51% to afforestation (for MAgPIE spatial C stocks were not available but afforestation is certainly much more important due to the limited decline in forest area in MAgPIE BASE). For BECCS, in both LUMs the CDR target was implemented as a gross CCS target which included the harvested C from bioenergy crops and a fractional (80%; Klein et al., 2014) capture and storage of this harvest. Cumulative CCS reaches 128 GtC in year 2099 in both LUMs (see subsection “Cumulative CCS”) so the implemented CDR/CCS target is achieved. However, calculations of the target in the LUMs originally neglected terrestrial C losses from deforestation for bioenergy cultivation. When these are included, cumulative CCS combined with ecosystem C losses from deforestation result in a net total C uptake of 86 and 107 GtC, thus below the sought target due to emissions from LUC.

In contrast to the two LUMs, total C uptake (relative to BASE) is typically lower in the DGVM simulations forced by the same LU patterns, with total C uptake in the DGVMs ranging between 19 and 130 GtC (Figs. 1a,b, 2a). Unsurprisingly (as LPJmL represents the vegetation component of the LUMs), the closest agreement exists between the LUMs and LPJmL. ORCHIDEE simulates the lowest uptake for ADAFF and JULES the lowest uptake for BECCS. The maximum yearly total C uptake per decade within the 21st century ranges from 1.9 GtC yr⁻¹ (IMAGE ADAFF) to 3.5 GtC yr⁻¹ (MAgPIE ADAFF) in the LUMs and from 0.4 GtC yr⁻¹ (ORCHIDEE IMAGE-ADAFF) to 2.0 GtC yr⁻¹ (LPJmL IMAGE-BECCS) in the DGVMs. Spatially, total C uptake is concentrated in the tropics for ADAFF (except in ORCHIDEE, which simulates substantial emissions in some regions), while patterns are more

diverse for BECCS (Fig. 3). The largest agreement in total C uptake across DGVMs is found in tropical Africa for the ADAFF scenarios (Fig. S4). The contributions of vegetation, soil, and cumulative CCS to model discrepancies in total C uptake are analyzed in the following subsections.

Vegetation carbon

As intended, the simulations with the ADAFF scenarios result in increasing biomass over the 21st century compared to the BASE simulations for all LUMs and DGVMs. Vegetation C uptake in year 2099 is 79 and 66 GtC in IMAGE and MAgPIE and ranges between 39 and 73 GtC in the DGVMs (Figs. 1c,d, 2b), with generally larger uptake for IMAGE scenarios than for MAgPIE scenarios due to the earlier start of ADAFF activities in IMAGE (Table S2). Biomass accumulation occurs at a relatively steady rate in the DGVMs but accelerates during the second half of the century in the LUMs (Fig. 1c,d). There is a drop in vegetation C for LPJmL MAgPIE-ADAFF around mid-century. As agricultural land has low vegetation C pools in LPJmL this is related to a decreasing vegetation C density in forests, which is not compensated for by the simultaneous increase in forest area. Tree PFTs in LPJmL are represented by average individuals (representing all trees belonging to this PFT), and the individual's properties are changed when afforestation occurs in a grid-cell. These changes in the PFT's properties might in some regions reduce its ability to compete or make it more vulnerable to disturbances so that tree mortality is increased compared to the BASE scenario in which no afforestation took place.

The vegetation C uptake in IMAGE can be equally attributed to avoided deforestation and to afforestation (Table S3). No quantification is possible in MAgPIE because spatial C stocks were not available. In the DGVMs, the contribution of avoided deforestation to the vegetation

C uptake in ADAFF is generally larger for IMAGE-LU than for MAgPIE-LU (Table S3), confirming the much larger role of afforestation compared to avoided deforestation in MAgPIE. For BECCS, all LUMs and DGVMs simulate deforestation-driven decreases in vegetation C. JULES simulates the largest biomass losses upon deforestation and ORCHIDEE the smallest losses. Since global vegetation C stocks are similar across DGVMs (with the exception of ORCHIDEE, Fig. S3), differences in C losses arise from spatial variations in biomass which DGVMs (and presumably LUMs) are known to not capture well (Johnson et al., 2016). BECCS deforestation emissions are generally larger for IMAGE-LU patterns than for MAgPIE-LU patterns, reflecting the much larger decline in forest area (Fig. S1, Table S2).

Site-level comparisons can help us to better understand differences across models. Therefore, in order to understand local responses better and to use these to interpret the simulated global totals, we extracted grid-cells from the global simulations (for IMAGE scenarios as spatial information were not available from MAgPIE), selected because a large fraction of the grid-cells' area underwent land-cover transitions within the 21st century. However, there are substantial variations in the models' response to LUC across different sites, making it difficult to choose representative grid-cells and to draw universal conclusions from this comparison. Figure S5 shows three relatively representative example sites. As expected for a 0.5° resolution, there are substantial differences on grid-cell level across models in terms of initial vegetation C densities. All models simulate increasing biomass in response to afforestation (Fig. S5a,b) and biomass losses upon deforestation (Fig. S5c). However, JULES does not simulate forest degradation (Fig. S5c; see methods for more information about degraded forests), contributing to the lower vegetation C uptake compared to the other DGVMs for the IMAGE ADAFF scenario.

For MAgPIE scenarios, site-level comparisons are not shown because MAgPIE only reported global C pools. For the MAgPIE ADAFF scenario, global vegetation C uptake is very similar

in all DGVMs but lower than in MAgPIE (Fig. 1d). It seems that one reason for this divergence is different assumptions about potential vegetation C stocks (available for MAgPIE and LPJ-GUESS; see Fig. S6). An additional factor explaining the divergence is the pace of the regrowth curve. In contrast to the other models, MAgPIE assumes a single response function per biome, irrespective of spatial differences in climate and soil conditions within a biome, and thus ignores the effects of spatial differences within a biome, e.g. in terms of annual precipitation or soil fertility on forest regrowth (Poorter *et al.*, 2016). Additionally, MAgPIE does not account for disturbances. When looking at forest regrowth rates averaged over different biomes it seems that tropical regrowth occurs much faster in MAgPIE than, for example, in LPJ-GUESS (Fig. S7a).

Soil carbon

Compared to vegetation, modelled soil C changes in response to ADAFF activities are much more diverse, with some DGVMs simulating net soil C losses upon afforestation (Figs. 1e,f, 2c). Soil C uptake in ADAFF is 62 GtC in IMAGE and 54 GtC in MAgPIE, which is comparable to vegetation C uptake. In contrast, soil C changes in the DGVMs range between -33 and +57 GtC. Soil C accumulation in LPJmL for the MAgPIE ADAFF scenario starts significantly earlier than in the other models. As afforestation on pastures is common in MAgPIE until around year 2070, this indicates a large soil C uptake potential in LPJmL for pasture-forests transitions, which is also apparent in the LPJmL simulations driven by the IMAGE ADAFF LU patterns. For BECCS, all models simulate small soil C losses (up to -16 GtC) which are generally larger in the LUMs than in the DGVMs. In both ADAFF and BECCS, differences between LUMs and DGVMs in terms of soil C changes are more pronounced for IMAGE-LU patterns than for MAgPIE-LU patterns.

336 The soil C emissions in JULES and ORCHIDEE for the ADAFF scenarios (and the relatively
337 low emissions for BECCS) might be partly caused by the simplistic representation of
338 agricultural management processes in these models. While LPJmL and LPJ-GUESS represent
339 croplands by specific crop PFTs and growing seasons, ORCHIDEE and JULES grow crops as
340 harvested grass (modified natural grass in ORCHIDEE, natural grass in JULES; see Table 1).
341 Additionally, ORCHIDEE does not include grazing of pastures, which means more biomass C
342 is transferred to the litter when the grass dies. Consequently, pastures and croplands have
343 larger soil C pools in ORCHIDEE and JULES, respectively, than if these processes were
344 accounted for, resulting in less soil C accumulation potential upon afforestation. To test
345 further how different representations of agriculture in the DGVMs affect soil C changes upon
346 afforestation we performed two sensitivity simulations with LPJ-GUESS in which we
347 simplified the representation of management processes following Pugh et al. (2015). In these
348 simulations, the rate of change in LPJ-GUESS soil C pools is reduced by 57% in the MAgPIE
349 ADAFF scenario (compared to the “standard” LPJ-GUESS simulations) when croplands are
350 represented by pastures (mimicking the representation of croplands in JULES), and by 49% in
351 the IMAGE ADAFF case when pastures are not harvested (mimicking the representation of
352 pastures in ORCHIDEE, not shown). Furthermore, LPJ-GUESS, JULES, and particularly
353 ORCHIDEE simulate a widespread decline in net primary productivity (NPP) upon
354 afforestation (Figs. 2f, S8) because in these models tropical grasslands (or croplands) are
355 often more productive than tropical forests. LPJmL, on the other hand, accounts for regional
356 yield gaps so cropland NPP is scaled down. Even though the fraction of NPP transferred to
357 the soil might differ across models (e.g. due to different mortality in secondary forests), this
358 suggests that the lower productivity of re-growing forests compared to agriculture also plays
359 an important role for the limited soil C accumulation (or emissions) in LPJ-GUESS, JULES,
360 and ORCHIDEE.

361

362 Cumulative CCS

363 CCS is calculated by multiplying the harvested C of bioenergy crops by a capture efficiency
364 of 80% before geologic storage. A prescribed CCS trajectory was implemented in both
365 LUMs, which means that annual global CCS rates are the same in IMAGE and MAgPIE.
366 Cumulative CCS reaches 128 GtC in both LUMs by year 2099. In the DGVMs, cumulative
367 CCS ranges from 37 to 130 GtC by year 2099 (Figs. 1g,h, 2d).

368 As the DGVMs used bioenergy production area from the LUMs and also the same
369 assumptions about capture efficiency and storage capacity, the lower CCS calculated in most
370 of the DGVMs has to arise mainly from differences in simulated bioenergy yields, including
371 differences in the harvest index. Both LUMs assume rain-fed perennial and fast-growing
372 second generation bioenergy crops (such as Miscanthus) to fulfil the CCS demand. LPJmL is
373 the only DGVM representing dedicated bioenergy crops explicitly, but like the other DGVMs
374 does not assume technological yield increases. This implies that the slightly larger cumulative
375 CCS than in MAgPIE originates from higher initial yields. In contrast, LPJ-GUESS grows
376 bioenergy as maize (with residues included for CCS), ORCHIDEE as crop grass, and JULES
377 as natural grass (for harvest assumptions see Table S1). Consequently, average bioenergy
378 yields are highest in LPJmL followed by LPJ-GUESS and then ORCHIDEE and JULES (Fig.
379 S9). Cumulative CCS in all DGVMs apart from LPJmL is higher for IMAGE-LU patterns
380 than for MAgPIE-LU patterns (Figs. 1g,h, 2d) because the larger cultivation area in IMAGE
381 (Fig. S2c,d) outweighs lower average yields (Fig. S9). In the LUMs, the same trade-off
382 between land expansion and yields results in equivalent global CCS rates in both LUMs.

383

384 Discussion

The C uptake potential of afforestation is largely restricted by historic C removal via deforestation. Cumulative LUC emissions over the 1750-2015 period were ~190 GtC (Le Quere et al., 2016), with a very large uncertainty arising from how different forms of land management are considered in the simulations (Arneth et al., 2017) but also due to different LUC hindcasts (Bayer et al., 2017). However, a possibly large fraction of agricultural area will be needed for future food production (Boysen *et al.*, 2017a, Popp *et al.*, 2017) and CO₂ fertilizing effects on forest growth will likely be limited in RCP2.6. This suggests that achieving 130 GtC net uptake via ADAFF might be challenging, consistent with results from the DGVMs here (especially for MAgPIE-LU where avoided deforestation only plays a minor role compared to afforestation). A limited (<150 GtC) C uptake potential via afforestation within this century was also estimated in previous studies, despite very different methods and assumptions (Lenton, 2010, and references therein). However, one recent study (Sonntag *et al.*, 2016) found a much larger (215 GtC) uptake in a coupled Earth System Model (ESM) for a high emission scenario (RCP8.5) when using RCP4.5 LU (afforestation, -700 Mha agricultural land) instead of RCP8.5 LU (deforestation, +800 Mha agricultural land). The C uptake was thus higher than in our study, but so were baseline deforestation rates, climate impacts, and, particularly, differences in CO₂ fertilization (RCP8.5 vs. RCP2.6 in our study); the high levels of CO₂ fertilization under RCP8.5 typically causes DGVMs to simulate much larger C uptake in forests.

Some of the discrepancy in total C uptake between the LUMs and the DGVMs in the ADAFF scenarios originates from differences in vegetation C uptake, especially for MAgPIE. Natural forest regrowth upon agricultural abandonment is implemented in all DGVMs and IMAGE, while MAgPIE assumes managed regrowth according to prescribed, region-specific growth curves towards the biomass density of potential natural vegetation (Humpenöder *et al.*, 2014). Observational studies differ substantially in reported forest regrowth rates (Krause *et al.*,

2016, and references therein). Biomass accumulation in tropical forests has often been reported to slow down a few decades after agricultural cessation, with aboveground biomass levels (representing ~80% of total biomass, Cairns *et al.*, 1997) of mature tropical forests being reached within ca. 66-90 years (Anderson-Teixeira *et al.*, 2016, Poorter *et al.*, 2016), and belowground biomass needing more time to recover, especially following shifting agriculture (Martin *et al.*, 2013). Poorter *et al.* (2016) also found slower accumulation rates in dry (<1500 mm) compared to wet (>2500 mm) environments. In comparison, tropical (22°S-20°N as in Poorter *et al.*) afforestation in the MAgPIE ADAFF scenario occurs in relatively dry regions, with an average precipitation of 1682 mm yr⁻¹. While we can only quantify tropical recovery times (90% of old forest biomass) for MAgPIE (47 years; Fig. S7a) and LPJ-GUESS (~150 years in tropical Africa), the vegetation C uptake is similar across all DGVMs. The observational studies point towards typical recovery times that lie in the middle of this range. This suggests that, assuming that afforestation will mostly occur as natural regrowth, tropical biomass accumulation rates might be overestimated in MAgPIE. The LPJ-GUESS recovery times of Krause *et al.* (2016) are, however, not directly comparable to these observations, as the LPJ-GUESS simulations allowed natural stand-replacing disturbances (e.g. fire, wind-throw) to occur in these recovering forests, slowing the recovery rate, whilst this is not likely to be the case in the chronosequence observations, which typically age the stand from last disturbance. Evaluation of forest regrowth rates in DGVMs, particularly in tropical forests, will be important to constrain uncertainty in ADAFF potential.

Degraded forests also represent an uncertainty in our IMAGE scenarios. JULES represented degraded forests as natural vegetation, whereas the other DGVMs, simply for consistency, followed the IMAGE assumption of degraded forests being grassland. In reality, degraded forests likely represents a mixture between both approaches, with aboveground biomass on average being 70% lower than in undisturbed forests (Asner *et al.*, 2010). Clearly, assuming a

degraded forest being a grassland will overestimate vegetation C uptake potential when degraded forests are converted back to forests (in IMAGE ~50% of the avoided deforestation and afforestation area by end-century is from degraded forests; see Table S2). Additionally, the mismatch between forest loss and agricultural gain reported by FAO (based on which the degraded forest class was introduced in IMAGE) might be largely explained by shifting cultivation (Houghton and Nassikas, 2017). However, most LUMs/DGVMs so far cannot adequately simulate shifting cultivation due to not explicitly representing forest demography. The representation of forest degradation thus remains a challenge for LUMs and DGVMs.

Soil C changes contribute most to variations in total C uptake across models. Differences in simulated present-day soil C stocks are hardly surprising as global soil C estimates are very uncertain (Scharlemann *et al.*, 2014) and large variations across DGVMs and ESMs have been reported before (Anav *et al.*, 2013, Tian *et al.*, 2015, Todd-Brown *et al.*, 2013). Numerous studies explored soil C changes following LUC (Smith *et al.*, 2016b, and references therein), but there is still substantial disagreement in terms of the magnitude of change for most land-cover transitions. While studies agree that transitions from forests to croplands reduce soil C (and vice versa), patterns are more diverse for conversions to/from grassland, depending on management intensity, climate, and soils (McSherry and Ritchie, 2013, Powers *et al.*, 2011). The picture is further complicated by evidence that the existing field observations in the tropics might not be representative for many tropical landscapes (Powers *et al.*, 2011).

The LUC scenarios from the LUMs differ in terms of converted land-cover types: in MAgPIE, afforestation partly takes place on former croplands (especially before year 2025 and after 2070). MAgPIE assumes initial litter C (both in croplands and pastures) to be completely depleted and, based on IPCC guidelines, to be replenished within 20 years following agricultural abandonment. Soil C in former croplands is assumed to increase from

the grid-cell specific average soil C density of cropland and natural vegetation towards the soil C density of natural vegetation within 20 years (Humpenöder *et al.*, 2014). However, a litter C density of zero and an assumed time frame of 20 years until soil C reaches equilibrium appear questionable. In fact, some studies report soil C to decrease during the first years after cropland cessation (Deng *et al.*, 2016), and subsequent C accumulation is usually slow and proceeds over several decades or even centuries (Silver *et al.*, 2000). In contrast to the prescribed recovery implemented in MAgPIE, IMAGE simulates soil C changes dynamically within LPJmL. However, the contribution of soils to total C uptake is comparable to MAgPIE even though ADAFF activities in IMAGE are largely restricted to pasture-forest transitions. In reality, afforestation on grasslands (or avoided conversion from forests to grasslands) has even less soil C uptake potential than on croplands; soil C depletions in pastures/grasslands relative to forests are generally low (Don *et al.*, 2011, Laganier *et al.*, 2010) and in many cases grasslands even store more soil C than the replacing forests (Li *et al.*, submitted; Guo and Gifford, 2002, Poeplau *et al.*, 2011, Powers *et al.*, 2011). Additionally, declines in soil C have been reported during the first years of forest regrowth before accumulation occurs and net accumulation is often only achieved after several decades (Paul *et al.*, 2002, Poeplau *et al.*, 2011). Consequently, the rapid soil C uptake in the LUMs for ADAFF is likely overoptimistic, while limited soil C accumulation (compared to vegetation C) in response to afforestation as simulated by some DGVMs seems to be more realistic. However, historic agriculture has likely resulted in substantial net soil C emissions (Sanderman *et al.*, 2017, Smith *et al.*, 2016b), so large soil C losses in response to afforestation as simulated by ORCHIDEE are also unlikely, especially for the MAgPIE ADAFF scenario (where croplands are preferentially afforested).

One likely reason for the large discrepancy in simulated soil C changes in response to afforestation is the simulated change in ecosystem productivity. Todd-Brown *et al.* (2013)

showed that soil C stocks in ESMs are closely coupled to simulated NPP. In our simulations, simulated changes in NPP in response to ADAFF activities are very different across models, which partly explains differences in soil C accumulation. Modelling work by DeFries (2002) suggests that regional impacts of LUC on NPP are highly variable, depending on management intensity and original vegetation cover, and that cropland productivity is higher compared to forests in temperate regions. The relatively high productivity of temperate crops seems to be confirmed for European studies (Ciais *et al.*, 2010, Luyssaert *et al.*, 2010), but estimates are highly dependent on the data source from which NPP is derived. In the tropics, observations suggest crop productivity at many locations to be lower than for forests (Cleveland *et al.*, 2015, Monfreda *et al.*, 2008). As afforestation in our scenarios is mostly concentrated in the tropics, the NPP decrease following afforestation in most DGVMs seems to be unrealistic.

A second potentially important reason for the large differences in simulated soil C uptake is different amounts of C removed from agricultural land. Soil C recovery following agricultural cessation has recently been simulated with a different version of LPJ-GUESS (croplands were represented by tilled, fertilized, and harvested grassland rather than specific crop PFTs) and showed reasonable agreement with observations (Krause *et al.*, 2016). ORCHIDEE and JULES represent fewer management processes and therefore may underestimate soil C uptake potential in ADAFF (but also losses in BECCS); the incorporation of harvest (not included in ORCHIDEE pastures) and the representation of crops by specific crop PFTs (including tillage), instead of grasses, substantially increases soil C depletions on agricultural land in LPJ-GUESS (Pugh *et al.*, 2015). However, there are also observations suggesting that moderately intensive grazing might actually increase soil C stocks in C4-dominated grasslands (McSherry and Ritchie, 2013, Navarrete *et al.*, 2016), a process the DGVMs likely do not capture well.

509 The LUMs did not include deforestation emissions ("carbon debt", Fargione *et al.*, 2008) in
510 their BECCS CDR target. This is a common procedure in BECCS scenarios (or at least LUC
511 emissions are often not separated from fossil fuel emissions, e.g. Smith *et al.*, 2016a). For two
512 bioenergy scenarios (600 and 800 Mha production area made available via either
513 deforestation or agricultural abandonment, RCP2.6 climate) comparable in terms of area and
514 climate changes to our scenarios, a modelling study by Wiltshire and Davies-Barnard (2015)
515 estimated vegetation C losses of 70 and 0 GtC and, using average depletions from Guo and
516 Gillford (2002), soil C losses of 20 and 60 GtC. In our simulations, vegetation and soil C
517 emissions are relatively small, but our study still confirms that these emissions should not be
518 neglected when considering bioenergy as an option to achieve negative emissions.

519 Cumulative CCS in BECCS differs substantially across models, ranging between 37 GtC and
520 130 GtC in the DGVMs, and reaching 128 GtC in both LUMs. By comparison, Wiltshire and
521 Davies-Barnard (2015) found 75 and 200 GtC for the two comparable scenarios, which is
522 similar to the 100-230 GtC range reported by Smith *et al.* (2016a) for IAM scenarios
523 consistent with the 2°C target. Recently, Boysen *et al.* (2017a) estimated land availability for
524 bioenergy production in LPJmL. They found that in the best case scenario, biomass
525 plantations on abandoned agricultural land could deliver up to 350 GtC by 2100 (but likely
526 much less), and potentially more if plantations would replace natural ecosystems. In our
527 study, bioenergy area was prescribed by the LUMs and differences in CCS across models
528 originate from simulated bioenergy crop yields. The LUMs and LPJmL represent these crops
529 as dedicated bioenergy crops, mimicking characteristics of perennial energy crops like
530 switchgrass or Miscanthus. Bioenergy yields in LPJmL have recently been evaluated against
531 observations and showed reasonable results but were hindered by limited experimental data in
532 the tropics (Heck *et al.*, 2016). The other DGVMs grow bioenergy crops as maize (LPJ-
533 GUESS), productive grass (ORCHIDEE), or natural grass (JULES). JULES and ORCHIDEE

also do not increase the harvest index for bioenergy crops relative to food crops. Additionally, the LUMs assume technological yield increases over time, resulting in higher average yields than in most DGVMs. While research of dedicated bioenergy crops is just in its infancy and thus on the one hand promises high potential, there is also evidence that yield increases observed over the last decades for cereals have recently slowed down (Alexandratos and Bruinsma, 2012). In fact, much of the historic yield increase was achieved via increasing the harvest index and fertilizer application, processes that are unlikely to substantially affect bioenergy yields (Searle and Malins, 2014). It also remains to be seen what bioenergy yield will be attainable in more marginal lands compared to sites where these crops are typically grown today (Searle and Malins, 2014). Consequently, what bioenergy yields we can expect in the future is controversial, with the optimistic assumptions made in IAMs/LUMs being plausible, but towards the upper bound of uncertainty (Creutzig, 2016).

We conclude that forest maintenance and expansion, as well as large-scale bioenergy production combined with CCS, offer the potential to remove substantial amounts of C from the atmosphere and thus can help to mitigate climate change. However, the size of the removal is highly uncertain, and may be much less than previously assumed in IAM/LUM scenarios consistent with the 2°C target (Boysen *et al.*, 2017b, Rogelj *et al.*, 2015, Smith *et al.*, 2016a, Tavoni and Socolow, 2013, Wiltshire and Davies-Barnard, 2015); the C uptake simulated by the LUMs is only achieved in one out of 16 combinations of mitigation LUC scenarios and DGVMs. The main reasons for the typically lower C uptake in the DGVMs as initially implemented in the LUMs are slower soil C accumulation (or even losses) following afforestation, different assumptions on potential vegetation C stocks, lower growth rates of forests, and lower bioenergy yields. Clearly the per-area C uptake (and thus the land demand) in land-based mitigation scenarios depends on assumptions made about vegetation and soil processes in the IAMs/LUMs. An improved implementation of land-based CDR options in

both kinds of models, LUMs and DGVMs, as well as a deeper interaction between both is necessary to draw more robust conclusions about the potential contribution of land management to climate stabilization. While the LUMs should emphasize the large uncertainty in assumed yields from bioenergy plantations, the DGVMs need to improve the parameterizations of managed herbaceous vegetation, particularly bioenergy crops (and also woody bioenergy), as well as regrowth of managed forests for afforestation. Field observations should focus on studying bioenergy crop productivity under commercial production conditions. Additionally, the LUMs and some DGVMs need to reconsider their assumptions about soil C sequestration rates following afforestation. More detailed information about grazing intensities on grasslands, and a clear differentiation between natural grasslands and intensively managed pastures in observational studies might also help to reduce the uncertainty in soil C changes following LUC (Navarrete *et al.*, 2016).

In this study we only address the uncertainty in land-based mitigation arising from potential C uptake for a prescribed available area. However, the establishment of negative emissions from land management could also be hindered by unacceptable social or ecological side-effects (Kartha and Dooley, 2016, Krause *et al.*, 2017, Smith *et al.*, 2016a), biophysical and biogeochemical climate impacts beyond C (Boysen *et al.*, 2017a, Krause *et al.*, 2017, Smith *et al.*, 2016a), irreversible effects of overshooting CO₂ concentrations (Kartha and Dooley, 2016, Tokarska and Zickfeld, 2015), or simply because CCS turns out to be technologically infeasible at commercial scale. There is also strong evidence that the timescales for shifts in farming systems to be realized may be of the order of several decades, substantially delaying the onset of negative emissions from BECCS (Alexander *et al.*, 2013; Brown *et al.*, submitted). Combining these unknowns and caveats with the large uncertainty in uptake potential identified in this study suggests that relying on negative emissions to mitigate climate change is a very high-risk strategy.

584

585 **Acknowledgements**

586 This work was funded by the Helmholtz Association through the International Research
587 Group CLUCIE and by the European Commission's Seventh Framework Programme, under
588 grant agreement number 603542 (LUC4C). Andreas Krause, Anita D. Bayer, and Almut
589 Arneth also acknowledge support by the European Commission's Seventh Framework
590 Programme, under grant agreement number 308393 (OPERAs). This work was supported, in
591 part, by the German Federal Ministry of Education and Research (BMBF), through the
592 Helmholtz Association and its research program ATMO. It also represents paper number 22
593 of the Birmingham Institute of Forest Research.

594

595 **Conflict of Interest**

596 The authors declare no conflict of interest.

597

598 **References**

- 599 Alexander P, Moran D, Rounsevell MDA, Smith P (2013) Modelling the perennial energy crop market:
600 the role of spatial diffusion. *Journal of the Royal Society Interface*, **10**,
601 doi:10.1098/Rsif.2013.0656.
- 602 Alexandratos N, Bruinsma J (2012) World agriculture towards 2030/2050: the 2012 revision. Rome,
603 FAO.
- 604 Anav A, Friedlingstein P, Kidston M *et al.* (2013) Evaluating the Land and Ocean Components of the
605 Global Carbon Cycle in the CMIP5 Earth System Models. *Journal of Climate*, **26**, 6801-6843,
606 doi:10.1175/Jcli-D-12-00417.1.
- 607 Anderson-Teixeira KJ, Wang MMH, Mcgarvey JC, Lebauer DS (2016) Carbon dynamics of mature and
608 regrowth tropical forests derived from a pantropical database (TropForC-db). *Global Change*
609 *Biology*, **22**, 1690-1709, doi:10.1111/gcb.13226.

610 Anderson K, Peters G (2016) The trouble with negative emissions. *Science*, **354**, 182-183,
611 doi:10.1126/science.aah4567.

612 Arneth A, Sitch S, Pongratz J *et al.* (2017) Historical carbon dioxide emissions caused by land-use
613 changes are possibly larger than assumed. *Nature Geoscience*, **10**, 79-84,
614 doi:10.1038/NGEO2882.

615 Asner GP, Powell GVN, Mascaro J *et al.* (2010) High-resolution forest carbon stocks and emissions in
616 the Amazon. *Proceedings of the National Academy of Sciences of the United States of*
617 *America*, **107**, 16738-16742, doi:10.1073/pnas.1004875107.

618 Bayer AD, Lindeskog M, Pugh TaM, Anthoni PM, Fuchs R, Arneth A (2017) Uncertainties in the land-
619 use flux resulting from land-use change reconstructions and gross land transitions. *Earth*
620 *System Dynamics*, **8**, 91-111, doi:10.5194/esd-8-91-2017.

621 Best MJ, Pryor M, Clark DB *et al.* (2011) The Joint UK Land Environment Simulator (JULES), model
622 description - Part 1: Energy and water fluxes. *Geoscientific Model Development*, **4**, 677-699,
623 doi:10.5194/gmd-4-677-2011.

624 Bondeau A, Smith PC, Zaehle S *et al.* (2007) Modelling the role of agriculture for the 20th century
625 global terrestrial carbon balance. *Global Change Biology*, **13**, 679-706, doi:10.1111/j.1365-
626 2486.2006.01305.x.

627 Boysen LR, Lucht W, Gerten D (2017a) Trade-offs for food production, nature conservation and
628 climate limit the terrestrial carbon dioxide removal potential. *Global Change Biology*,
629 doi:10.1111/gcb.13745.

630 Boysen LR, Lucht W, Gerten D, Heck V, Lenton TM, Schellnhuber HJ (2017b) The limits to global-
631 warming mitigation by terrestrial carbon removal. *Earths Future*, **5**, 463-474,
632 doi:10.1002/2016EF000469.

633 Cairns MA, Brown S, Helmer EH, Baumgardner GA (1997) Root biomass allocation in the world's
634 upland forests. *Oecologia*, **111**, 1-11, doi:10.1007/s004420050201.

635 Ciais P, Wattenbach M, Vuichard N *et al.* (2010) The European carbon balance. Part 2: croplands.
636 *Global Change Biology*, **16**, 1409-1428, doi:10.1111/j.1365-2486.2009.02055.x.

637 Clark DB, Mercado LM, Sitch S *et al.* (2011) The Joint UK Land Environment Simulator (JULES), model
638 description - Part 2: Carbon fluxes and vegetation dynamics. *Geoscientific Model*
639 *Development*, **4**, 701-722, doi:10.5194/gmd-4-701-2011.

640 Cleveland CC, Taylor P, Chadwick KD *et al.* (2015) A comparison of plot-based satellite and Earth
641 system model estimates of tropical forest net primary production. *Global Biogeochemical*
642 *Cycles*, **29**, 626-644, doi:10.1002/2014GB005022.

643 Creutzig F (2016) Economic and ecological views on climate change mitigation with bioenergy and
644 negative emissions. *Global Change Biology Bioenergy*, **8**, 4-10, doi:10.1111/gcbb.12235.

645 Defries R (2002) Past and future sensitivity of primary production to human modification of the
646 landscape. *Geophysical Research Letters*, **29**, doi:10.1029/2001gl013620.

647 Deng L, Zhu G, Tang Z, Shangguan Z (2016) Global patterns of the effects of land-use changes on soil
648 carbon stocks. *Global Ecology and Conservation*, **5**, 127-138,
649 doi:10.1016/j.gecco.2015.12.004.

650 Doelman JC, Stehfest E, Tabeau A *et al.* (2018) Exploring SSP land-use dynamics using the IMAGE
651 model: Regional and gridded scenarios of land-use change and land-based climate change
652 mitigation. *Global Environmental Change*, **48**, 119-135, doi:10.1016/j.gloenvcha.2017.11.014.

653 Don A, Schumacher J, Freibauer A (2011) Impact of tropical land-use change on soil organic carbon
654 stocks - a meta-analysis. *Global Change Biology*, **17**, 1658-1670, doi:10.1111/j.1365-
655 2486.2010.02336.x.

656 Fargione J, Hill J, Tilman D, Polasky S, Hawthorne P (2008) Land clearing and the biofuel carbon debt.
657 *Science*, **319**, 1235-1238, doi:10.1126/science.1152747.

658 Fuss S, Canadell JG, Peters GP *et al.* (2014) COMMENTARY: Betting on negative emissions. *Nature*
659 *Climate Change*, **4**, 850-853, doi:10.1038/nclimate2392.

660 Gasser T, Guivarch C, Tachiiri K, Jones CD, Ciais P (2015) Negative emissions physically needed to
661 keep global warming below 2 degrees C. *Nature Communications*, **6**,
662 doi:10.1038/Ncomms8958.

663 Guo LB, Gifford RM (2002) Soil carbon stocks and land use change: a meta analysis. *Global Change*
664 *Biology*, **8**, 345-360, doi:10.1046/j.1354-1013.2002.00486.x.

665 Heck V, Gerten D, Lucht W, Boysen LR (2016) Is extensive terrestrial carbon dioxide removal a 'green'
666 form of geoengineering? A global modelling study. *Global and Planetary Change*, **137**, 123-
667 130, doi:10.1016/j.gloplacha.2015.12.008.

668 Hempel S, Frieler K, Warszawski L, Schewe J, Piontek F (2013) A trend-preserving bias correction - the
669 ISI-MIP approach. *Earth System Dynamics*, **4**, 219-236, doi:10.5194/esd-4-219-2013.

670 Houghton RA, Nassikas AA (2017) Negative emissions from stopping deforestation and forest
671 degradation, globally. *Global Change Biology*, 1-10, doi:10.1111/gcb.13876.

672 Humpenöder F, Popp A, Dietrich JP *et al.* (2014) Investigating afforestation and bioenergy CCS as
673 climate change mitigation strategies. *Environmental Research Letters*, **9**, doi:10.1088/1748-
674 9326/9/6/064029.

675 Johnson MO, Galbraith D, Gloor M *et al.* (2016) Variation in stem mortality rates determines patterns
676 of above-ground biomass in Amazonian forests: implications for dynamic global vegetation
677 models. *Global Change Biology*, **22**, 3996-4013, doi:10.1111/gcb.13315.

678 Kartha S, Dooley K (2016) The risks of relying on tomorrow's 'negative emissions' to guide today's
679 mitigation action. Stockholm Environment Institute.

680 Klein D, Luderer G, Kriegler E *et al.* (2014) The value of bioenergy in low stabilization scenarios: an
681 assessment using REMIND-MAGPIE. *Climatic Change*, **123**, 705-718, doi:10.1007/s10584-013-
682 0940-z.

683 Klein Goldewijk K, Beusen A, Van Dreht G, De Vos M (2011) The HYDE 3.1 spatially explicit database
684 of human-induced global land-use change over the past 12,000 years. *Global Ecology and*
685 *Biogeography*, **20**, 73-86, doi:10.1111/j.1466-8238.2010.00587.x.

686 Krause A, Pugh TaM, Bayer AD *et al.* (2017) Global consequences of afforestation and bioenergy
687 cultivation on ecosystem service indicators. *Biogeosciences*, **14**, 4829–4850, doi:10.5194/bg-
688 14-4829-2017.

689 Krause A, Pugh TaM, Bayer AD, Lindeskog M, Arneth A (2016) Impacts of land-use history on the
690 recovery of ecosystems after agricultural abandonment. *Earth System Dynamics*, **7**, 745-766,
691 doi:10.5194/esd-7-745-2016.

692 Krinner G, Viovy N, De Noblet-Ducoudre N *et al.* (2005) A dynamic global vegetation model for
693 studies of the coupled atmosphere-biosphere system. *Global Biogeochemical Cycles*, **19**,
694 doi:10.1029/2003gb002199.

695 Laganier J, Angers DA, Pare D (2010) Carbon accumulation in agricultural soils after afforestation: a
696 meta-analysis. *Global Change Biology*, **16**, 439-453, doi:10.1111/j.1365-2486.2009.01930.x.

697 Le Quere C, Andrew RM, Canadell JG *et al.* (2016) Global Carbon Budget 2016. *Earth System Science*
698 *Data*, **8**, 605-649, doi:10.5194/essd-8-605-2016.

699 Lenton TM (2010) The potential for land-based biological CO₂ removal to lower future atmospheric
700 CO₂ concentration. *Carbon Management*, **1**, 145-160, doi:10.4155/Cmt.10.12.

701 Lenton TM, Vaughan NE (2009) The radiative forcing potential of different climate geoengineering
702 options. *Atmospheric Chemistry and Physics*, **9**, 5539-5561, doi:10.5194/acp-9-5539-2009.

703 Lotze-Campen H, Muller C, Bondeau A, Rost S, Popp A, Lucht W (2008) Global food demand,
704 productivity growth, and the scarcity of land and water resources: a spatially explicit
705 mathematical programming approach. *Agricultural Economics*, **39**, 325-338,
706 doi:10.1111/j.1574-0862.2008.00336.x.

707 Luysaert S, Ciais P, Piao SL *et al.* (2010) The European carbon balance. Part 3: forests. *Global Change*
708 *Biology*, **16**, 1429-1450, doi:10.1111/j.1365-2486.2009.02056.x.

709 Martin PA, Newton AC, Bullock JM (2013) Carbon pools recover more quickly than plant biodiversity
710 in tropical secondary forests. *Proceedings of the Royal Society B-Biological Sciences*, **280**,
711 doi:10.1098/Rspb.2013.2236.

712 Mcsherry ME, Ritchie ME (2013) Effects of grazing on grassland soil carbon: a global review. *Global*
713 *Change Biology*, **19**, 1347-1357, doi:10.1111/gcb.12144.

714 Meinshausen M, Smith SJ, Calvin K *et al.* (2011) The RCP greenhouse gas concentrations and their
715 extensions from 1765 to 2300. *Climatic Change*, **109**, 213-241, doi:10.1007/s10584-011-
716 0156-z.

717 Monfreda C, Ramankutty N, Foley JA (2008) Farming the planet: 2. Geographic distribution of crop
718 areas, yields, physiological types, and net primary production in the year 2000. *Global*
719 *Biogeochemical Cycles*, **22**, doi:10.1029/2007gb002947.

720 Navarrete D, Sitch S, Aragao LEOC, Pedroni L (2016) Conversion from forests to pastures in the
721 Colombian Amazon leads to contrasting soil carbon dynamics depending on land
722 management practices. *Global Change Biology*, **22**, 3503-3517, doi:10.1111/gcb.13266.

723 Olin S, Lindeskog M, Pugh TaM *et al.* (2015) Soil carbon management in large-scale Earth system
724 modelling: implications for crop yields and nitrogen leaching. *Earth System Dynamics*, **6**, 745-
725 768, doi:10.5194/esd-6-745-2015.

726 Paul KI, Polglase PJ, Nyakuengama JG, Khanna PK (2002) Change in soil carbon following
727 afforestation. *Forest Ecology and Management*, **168**, 241-257, doi:10.1016/S0378-
728 1127(01)00740-X.

729 Poeplau C, Don A, Vesterdal L, Leifeld J, Van Wesemael B, Schumacher J, Gensior A (2011) Temporal
730 dynamics of soil organic carbon after land-use change in the temperate zone - carbon
731 response functions as a model approach. *Global Change Biology*, **17**, 2415-2427,
732 doi:10.1111/j.1365-2486.2011.02408.x.

733 Poorter L, Ongers FB, Aide TM *et al.* (2016) Biomass resilience of Neotropical secondary forests.
734 *Nature*, **530**, 211-214, doi:10.1038/nature16512.

735 Popp A, Calvin K, Fujimori S *et al.* (2017) Land-use futures in the shared socio-economic pathways.
736 *Global Environmental Change-Human and Policy Dimensions*, **42**, 331-345,
737 doi:10.1016/j.gloenvcha.2016.10.002.

738 Popp A, Humpenoder F, Weindl I *et al.* (2014a) Land-use protection for climate change mitigation.
739 *Nature Climate Change*, **4**, 1095-1098, doi:10.1038/Nclimate2444.

740 Popp A, Rose SK, Calvin K *et al.* (2014b) Land-use transition for bioenergy and climate stabilization:
741 model comparison of drivers, impacts and interactions with other land use based mitigation
742 options. *Climatic Change*, **123**, 495-509, doi:10.1007/s10584-013-0926-x.

743 Powers JS, Corre MD, Twine TE, Veldkamp E (2011) Geographic bias of field observations of soil
744 carbon stocks with tropical land-use changes precludes spatial extrapolation. *Proceedings of*
745 *the National Academy of Sciences of the United States of America*, **108**, 6318-6322,
746 doi:10.1073/pnas.1016774108.

747 Pugh TaM, Arneth A, Olin S *et al.* (2015) Simulated carbon emissions from land use change are
748 substantially enhanced by accounting for agricultural management. *Environmental Research*
749 *Letters*, **10**, doi:10.1088/1748-9326/10/12/124008.

750 Riahi K, Van Vuuren DP, Kriegler E *et al.* (2017) The Shared Socioeconomic Pathways and their
751 energy, land use, and greenhouse gas emissions implications: An overview. *Global*
752 *Environmental Change-Human and Policy Dimensions*, **42**, 153-168,
753 doi:10.1016/j.gloenvcha.2016.05.009.

754 Rogelj J, Luderer G, Pietzcker RC, Kriegler E, Schaeffer M, Krey V, Riahi K (2015) Energy system
755 transformations for limiting end-of-century warming to below 1.5 degrees C. *Nature Climate*
756 *Change*, **5**, 519–527, doi:10.1038/nclimate2572.

757 Sanderman J, Hengl T, Fiske GJ (2017) Soil carbon debt of 12,000 years of human land use.
 758 *Proceedings of the National Academy of Sciences of the United States of America*, **114**, 9575-
 759 9580, doi:10.1073/pnas.1706103114.

760 Sanderson BM, O'Neill BC, Tebaldi C (2016) What would it take to achieve the Paris temperature
 761 targets? *Geophysical Research Letters*, **43**, 7133-7142, doi:10.1002/2016GL069563.

762 Scharlemann JPW, Tanner EVJ, Hiederer R, Kapos V (2014) Global soil carbon: understanding and
 763 managing the largest terrestrial carbon pool. *Carbon Management*, **5**, 81-91,
 764 doi:10.4155/Cmt.13.77.

765 Searle SY, Malins CJ (2014) Will energy crop yields meet expectations? *Biomass & Bioenergy*, **65**, 3-
 766 12, doi:10.1016/j.biombioe.2014.01.001.

767 Silver WL, Ostertag R, Lugo AE (2000) The potential for carbon sequestration through reforestation of
 768 abandoned tropical agricultural and pasture lands. *Restoration Ecology*, **8**, 394-407,
 769 doi:10.1046/j.1526-100x.2000.80054.x.

770 Sitch S, Smith B, Prentice IC *et al.* (2003) Evaluation of ecosystem dynamics, plant geography and
 771 terrestrial carbon cycling in the LPJ dynamic global vegetation model. *Global Change Biology*,
 772 **9**, 161-185, doi:10.1046/j.1365-2486.2003.00569.x.

773 Smith B, Warlind D, Arneth A, Hickler T, Leadley P, Siltberg J, Zaehle S (2014) Implications of
 774 incorporating N cycling and N limitations on primary production in an individual-based
 775 dynamic vegetation model. *Biogeosciences*, **11**, 2027-2054, doi:10.5194/bg-11-2027-2014.

776 Smith P, Davis SJ, Creutzig F *et al.* (2016a) Biophysical and economic limits to negative CO₂ emissions.
 777 *Nature Climate Change*, **6**, 42-50, doi:10.1038/Nclimate2870.

778 Smith P, House JI, Bustamante M *et al.* (2016b) Global change pressures on soils from land use and
 779 management. *Global Change Biology*, **22**, 1008-1028, doi:10.1111/gcb.13068.

780 Sonntag S, Pongratz J, Reick CH, Schmidt H (2016) Reforestation in a high-CO₂ world-Higher
 781 mitigation potential than expected, lower adaptation potential than hoped for. *Geophysical
 782 Research Letters*, **43**, 6546-6553, doi:10.1002/2016GL068824.

783 Stehfest E, Van Vuuren D, Kram T *et al.* (2014) Integrated Assessment of Global Environmental
 784 Change with IMAGE 3.0 : Model description and policy applications. The Hague: PBL
 785 Netherlands Environmental Assessment Agency.

786 Tavoni M, Socolow R (2013) Modeling meets science and technology: an introduction to a special
 787 issue on negative emissions. *Climatic Change*, **118**, 1-14, doi:10.1007/s10584-013-0757-9.

788 Tian HQ, Lu CQ, Yang J *et al.* (2015) Global patterns and controls of soil organic carbon dynamics as
 789 simulated by multiple terrestrial biosphere models: Current status and future directions.
 790 *Global Biogeochemical Cycles*, **29**, 775-792, doi:10.1002/2014GB005021.

791 Todd-Brown KEO, Randerson JT, Post WM, Hoffman FM, Tarnocai C, Schuur EaG, Allison SD (2013)
 792 Causes of variation in soil carbon simulations from CMIP5 Earth system models and
 793 comparison with observations. *Biogeosciences*, **10**, 1717-1736, doi:10.5194/bg-10-1717-
 794 2013.

795 Tokarska KB, Zickfeld K (2015) The effectiveness of net negative carbon dioxide emissions in reversing
796 anthropogenic climate change. *Environmental Research Letters*, **10**, doi:10.1088/1748-
797 9326/10/9/094013.

798 Williamson P (2016) Scrutinize CO2 removal methods. *Nature*, **530**, 153-155, doi:10.1038/530153a.

799 Wiltshire A, Davies-Barnard T (2015) Planetary limits to BECCS negative emissions. In: *AVOID 2*
800 *WPD.2a Report 1*.

801

802

803

804

805

806

807

808

809

810

811

812

813

814

816 Table 1: Overview of major DGVM differences relevant to this study. A more detailed
 817 version of the table can be found in the supplement (Table S1).

Variable or process	DGVM			
	LPJ-GUESS	ORCHIDEE	JULES	LPJmL
Spatial resolution	0.5° x 0.5°	2° x 2°	0.5° x 0.5°	
Nitrogen cycle	yes	no		
Implementation of LU patterns from the LUMs into the DGVM	absolute cropland, pasture, and natural area prescribed by LUMs, PFT distribution on natural land is simulated dynamically	changes in cropland, pasture, and forest vs. other natural area prescribed by LUMs, forest area and PFT distribution (static on natural land) in year 2005 according to internal map (from European Space Agency)	absolute cropland, pasture, and natural area prescribed by LUMs, PFT distribution on natural land is simulated dynamically	
Implementation of agricultural expansion	all natural PFTs are reduced proportionally		grasslands are reduced first, then shrubs, then forests	all natural PFTs are reduced proportionally
Representation of degraded forests (for IMAGE-LU patterns only)	as pasture	as natural grassland	as natural vegetation (forests or natural grassland)	as pasture
Forest (re)growth dynamics	cohort approach (competition between different age classes), natural regrowth	dilution approach (one average individual per PFT), natural regrowth		
Pasture management	harvest, woody vegetation is prevented from growing	no harvest, woody vegetation is prevented from growing	harvest*, woody vegetation is prevented from growing	harvest with variable intensity, woody vegetation is prevented from

				growing
Cropland management	four crop PFTs (temperate wheat, maize, rice, temperate other), variable sowing and harvest date, tillage, irrigation, fertilization, dynamic potential heat unit calculation, woody vegetation is prevented from growing	C3 + C4 crop grass (similar phenology as natural grass but adapted maximum LAI and slightly modified critical temperature and humidity parameters), harvest, woody vegetation is prevented from growing	C3 + C4 grass, harvest, woody vegetation is prevented from growing	12 crop PFTs, variable sowing and harvest date, irrigation, woody vegetation is prevented from growing
Dedicated bioenergy crop PFTs	no (grown as maize)	no (grown as C3 or C4 crop grass)	no (grown as C3 or C4 grass)	yes (fast-growing C4 grass, temperate and tropical short rotation coppices)

*Pastures were treated as cropland in these JULES simulations. Normally pastures are not harvested in JULES.

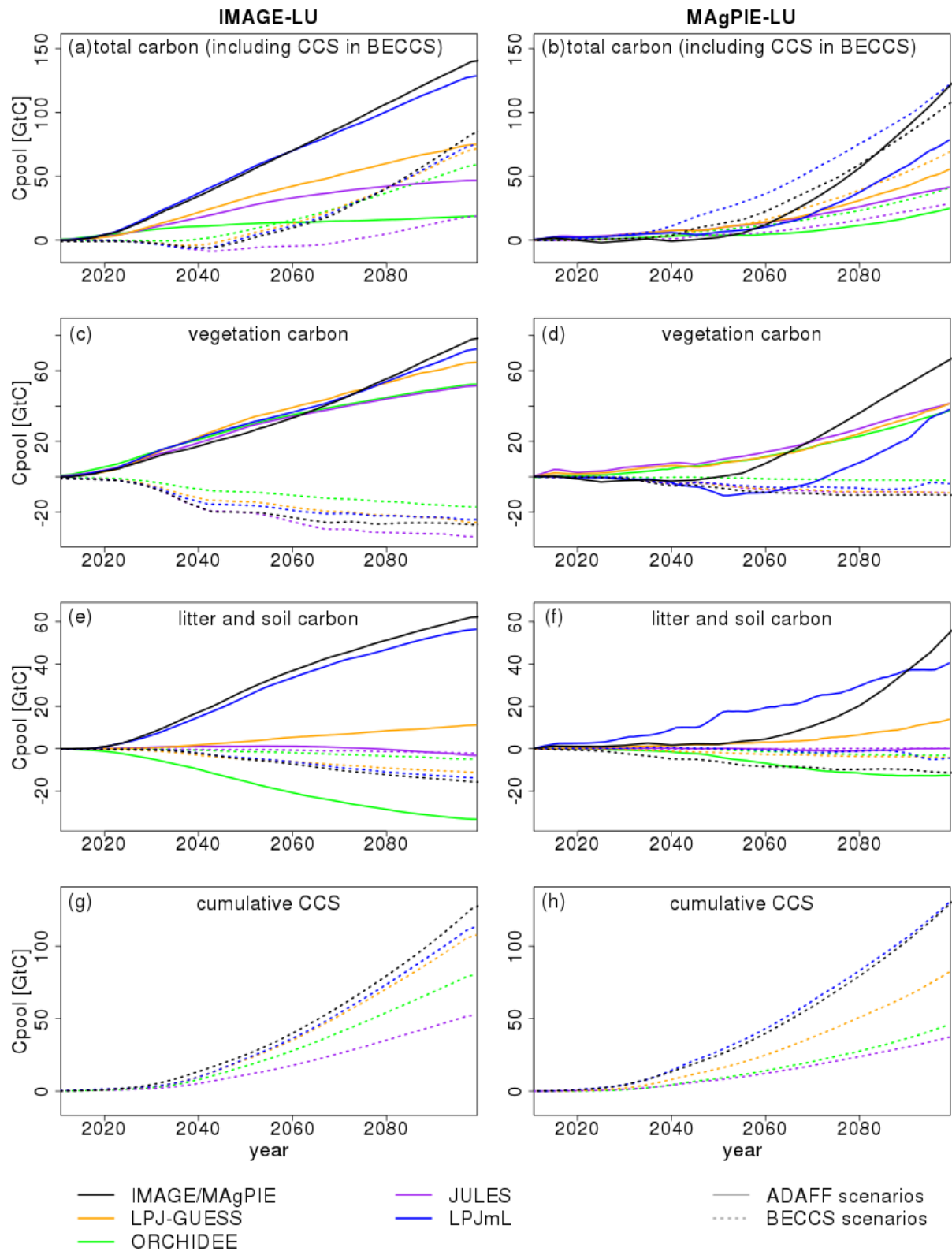


Figure 1: Time-series (2010-2099) of simulated C uptake (total of all grid-cells) in the LUMs and DGVMs for the mitigation simulations (compared to the respective BASE simulation), for IMAGE-LU patterns (left, 5-year running means) and MAgPIE-LU patterns (right). a+b) total C (including cumulative CCS), c+d) vegetation C, e+f) litter and soil C, g+h) cumulative CCS.

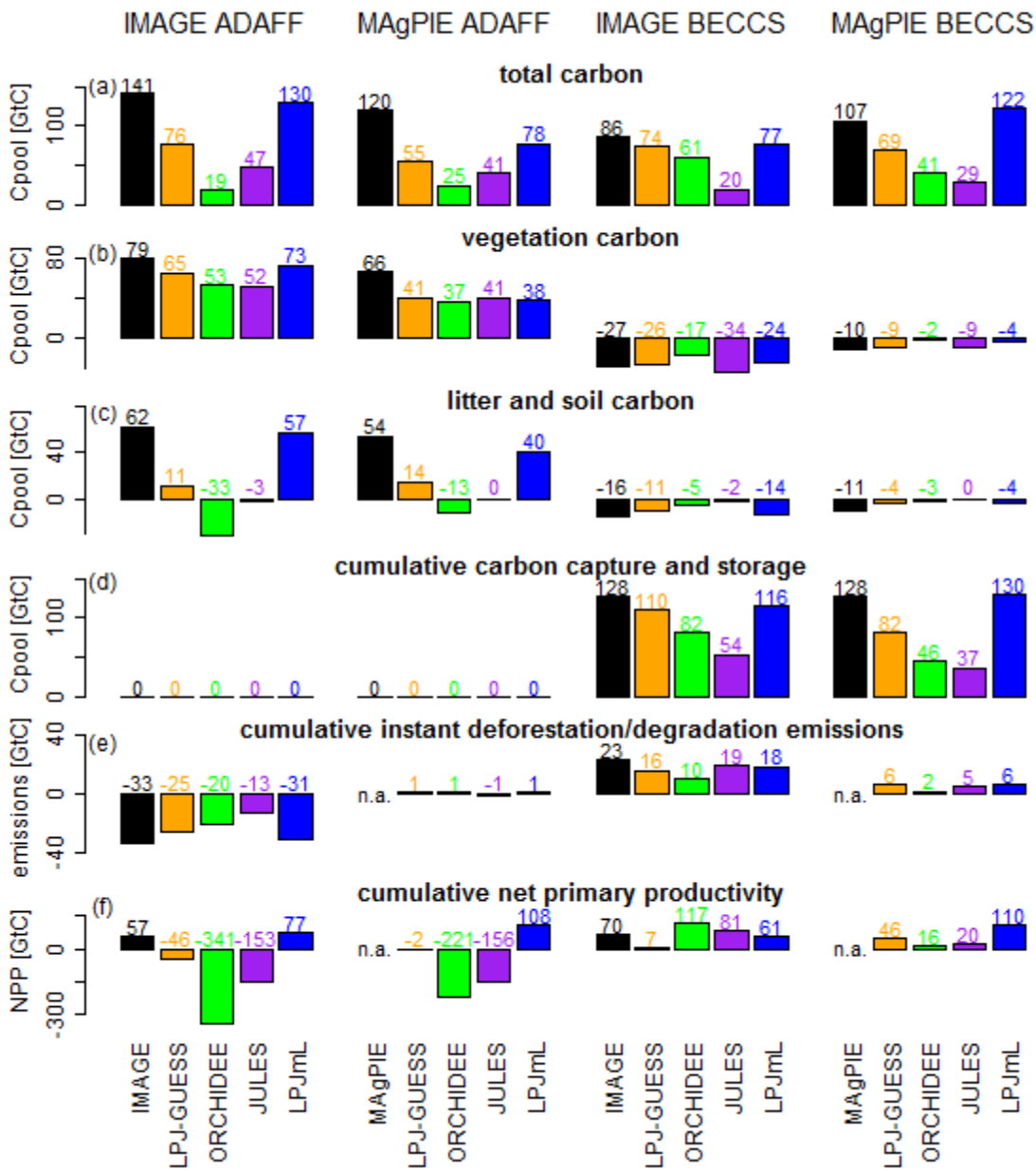


Figure 2: Simulated change in total C (a), vegetation C (b), litter and soil C (c), cumulative CCS (d), cumulative instant (oxidized in the same year) deforestation/degradation emissions (e), and cumulative NPP (f) between year 2005 and 2009 for the mitigation simulations (compared to the respective BASE simulation) in IMAGE/MAGPIE (as simulated by the LUMs in the LUC scenarios), LPJ-GUESS, ORCHIDEE, JULES and LPJmL.

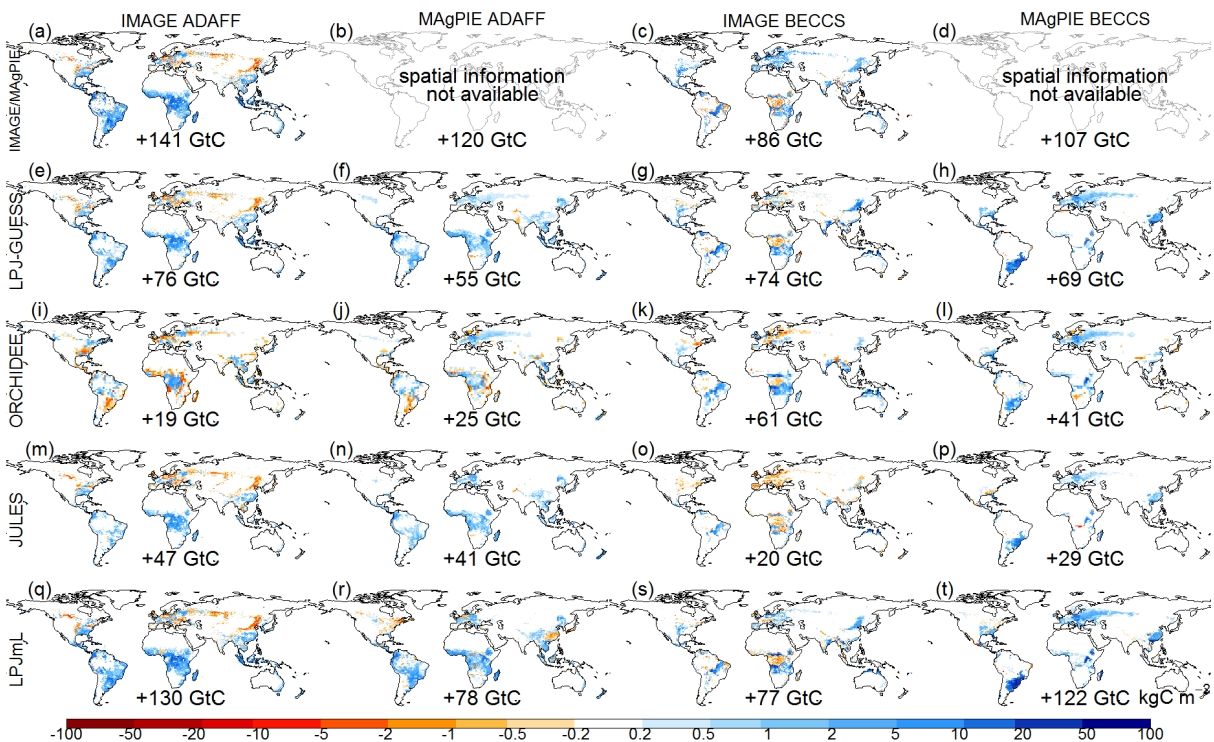


Figure 3: Spatial distribution of total C uptake in the LUMs (a-d) and DGVMs (e-t) for the mitigation scenarios (compared to BASE) between year 2005 and 2009 for IMAGE ADAFF (1st column), MAGPIE ADAFF (2nd column), IMAGE BECCS (3rd column) and MAGPIE BECCS (4th column). Numbers are global totals.